CYBERNETICS AND PHYSICS, VOL. 13, NO. 3, 2024, 211–219

ANTI-RESONANCE IN THE SYSTEMS OF NONLINEAR OSCILLATORS

Margarita A. Kovaleva
Polymer Department
N.N.Semenov Federal Research Centre
for Chemical Physics RAS
Russia
makovaleva@chph.ras.ru
Physics Department
HSE University
Russia

Valeri V. Smirnov
Polymer Department
N.N.Semenov Federal Research Centre
for Chemical Physics RAS
Russia
vvs@polymer.chph.ras.ru

Article history:
Received 15.10.2024, Accepted 12.11.2024

Abstract

The anti-resonance phenomenon analogous to the Fano resonance in the classical system of two oscillators with nonlinearity is observed. The focus of the work is on the effects of nonlinearity in the system. The explicit form of the solution for the full nonlinear problem is obtained for the arbitrary type of the nonlinearity and in a wide range of the parameters. The results of the analytical study show very good agreement with the data of the direct numerical simulations. The peculiarities resulted from the multiplicity of the solutions are discussed. The paper was presented at PhysCon2024

Key words

Anti-resonance, Fano resonance, nonlinear oscillators, destructive interference, stability of oscillation, complex envelope variable approximation

1 Introduction

The vibrations appear in a wide range of natural phenomena and technical processes. In the majority of the processes they are the basis of the object's functionality. Therefore the interest to the study of the vibrations does not decrease during decades. Interaction of some object with periodic or aperiodic external field was the basis of the consideration for many models and real systems[Neishtadt1 et al.(2013)Neishtadt1, Vasiliev and Artemyev]. Many different approaches were developed for the analysis: concept of non-linear normal modes[Albu-Schäffer and Della Santina(2020)], resonant manifold approach[Perchikov and Gendelman(2024)], limiting phase trajectory concept [Manevitch(2007); Manevitch and Smirnov(2010); Kovaleva et al.(2019)Kovaleva, Manevitch and Romeo] and the feedback control algorithm based on speed-gradient approach[Usik et al.(2024)Usik, Amelina and Fradkov]. As it is known, the main characteristics of the vibrations are the amplitude and the phase. The phase plays a crucial role in the processes of the interactions of the vibrations. It provides the existence of the interference phenomenon, which can be a constructive process as well as a destructive one. The latter may lead to the quenching of the oscillations. One of most famous effect, which results from the destructive interference in the quantum-mechanical systems, is Fano resonance, which is specific for the asymmetrical profile of the resonant amplitude-frequency response. The problem of the asymmetric resonant profile appeared for the first time in the study on the adsorption in the noble gases at the short wavelength (ultraviolet) edge of the spectrum [Beutler(1935)]. Ugo Fano, who was the postgraduate student by E.Fermi, explained this phenomenon by the resonant interaction of the discrete state with the wide non-resonant spectrum [Fano(1935)]. Later this problem was studied in the context of the electron scattering on the He atoms. The original work by U.Fano [Fano(1961)] became one of most cited papers in Physics during the following decades. The mechanism of the formation of the asymmetric resonant amplitude profile results from the destructive interference of the wave functions coupled with the continuum with the wave function of the discrete leaky state with a limited life-time. The processes of the destructive interference are of a very general character and have been intensively used in the contemporary spectroscopic

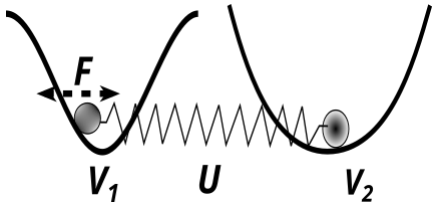

Figure 1. The system of two coupled particles in the potential wells V_1 and V_2, the coupling is shown as the spring U. The external field F acts on the left particle only.

investigations in the area of solid state physics and quantum electronics [Kosevich(2008); Kim et al.(2005)Kim, Lee, Kim and Ihm; M.F. et al.(2017)M.F., Rybin, Poddubny and Kivshar; Wang et al.(2016)Wang, Huang, Yao and Xu; Xu et al.(2018)Xu, Zhao, Chen and et al; Savin and Kivshar(2017)].

This type of resonance can be observed in the photonic structures of the microresonators associated with the waveguide. The system can be illustrated by the photonic crystals with partially reflective elements(defects). In the processes of collision and scattering of two particles, it is also possible to observe Fano resonances arising from the interference of unbounded states of particles (continuum) and quasi-bounded states. The review of the problems and the advances in the field may be found in the papers by Miroshnichenko and Kivshar [Miroshnichenko et al.(2010)Miroshnichenko, Flach and Kivshar; Kivshar(2018)].

The process of the destructive interference in the classic systems is called the anti-resonance. There is a number of papers, where the analogy between the quantum-mechanics and classical problems is discussed [Joe et al.(2006)Joe, Satanin and Kim; Riffe(2011); Lebedev and Misochko(2022)]. It was shown that a simplest classical model that demonstrates the asymmetric resonant profile is the system of two coupled oscillators with close eigenfrequencies, one of them subject to external harmonic forcing. In spite of the fact that the analogy is not complete, the main peculiarities are very close. The main differences between the quantum-mechanical and classical systems has been discussed by Lebedev and Misochko [Lebedev and Misochko(2022)]. The authors pointed out the non-conservative character of the classical systems and the principal linearity in the quantum-mechanical formulation of the problem. Indeed, the resonance phenomenon is specified by a significant growth of the amplitude of oscillations in the vicinity of the some specific frequency of the external forcing. This fact can lead to a significant rise of the role of non-linear effects. In such a case one should consider the amplitude-dependent eigenfrequency of the oscillator for the accurate description of the resonance.

The effect of the nonlinearity on the Fano resonance has been considered in [Kroner et al.(2008)Kroner, Govorov, Remi and et al.; Miroshnichenko(2009)], while the destructive interference of the wave in the one-dimensional chain with the nonlinear defect has been studied by Koroleva and Kosevich [Koroleva(Kikot) and Kosevich(2023)]. However, the closed equation for nonlinear system with a general type of the nonlinearity was not obtained yet. In our previous work the nonlinear system similar to the one considered in paper by Joe [Joe et al.(2006)Joe, Satanin and Kim], but comprising one nonlinear oscillator has been considered. The approximation used in the work allowed to obtain the transcendental equation for the amplitudes and phases of oscillator. The good agreement between the analytical results ans numerical simulation data has been demonstrated. It was shown that even the presence of a weak nonlinearity of one oscillator changes the behaviour of the system significantly. The algorithm for the estimation of the amplitude change when the jump between the different branches of the nonlinear amplitude-frequency characteristic occurs was been developed. Moreover, it was shown that there are some areas on the frequency-amplitude plane,where the motion of the oscillator becomes unstable and the evolution is analogous to a beating process.

The present paper presents the development of the previous work [Smirnov(2022)]. It contains the study of the system with non-linear coupling between oscillators and the systems with two nonlinear oscillators of a general type of nonlinearity. It turns out that in the contrast with the previous considerations the nonlinear coupling affects the high-frequency resonant response only, while the low-frequency response looks like the linear analogue. The frequency when the switch between different branches of the amplitude-frequency curves occurs can be determined in the framework of the Limiting Phase Trajectory concept [Manevitch(2007)]. The system with double nonlinearity (for the forced and the driven oscillators) is considered for soft as well as hard types of nonlinearity. We show that the most interesting situation arises when the types of the nonlinearity for two oscillators are different. In such a case we can observe the double jumps between different branches of two different solutions for the amplitudes of oscillators. The paper is organized as follows. Section 2 presents the model under consideration. Section 3 contains the analysis of the resonance of two linear oscillators with the nonlinear coupling. Section 4 is devoted to the study of the double nonlinear system, i.e. the system of two nonlinear oscillators with linear coupling. We discuss the results and the possible developments of the problem in Conclusions section.

2 The Model

We consider the system of two coupled oscillators shown in Fig. 1 . In the paper we will assume the different types of the potential wells V_1 and V_2, and coupling U. For the clarity Fig. 1 shows the potential well of the soft type (V_1) and the hard type (V_2). We would like to consider a general form of the potential well, however,

for the numerical realization of nonlinear oscillators we will use the potential $V(z) \sim 1 - \cos z$ for the soft type of nonlinearity and $V(z) \sim \cosh z - 1$ for the hard one. We assume that the oscillators have the unit masses and potential functions V_j are characterized by parameters Ω_j, which are proportional to the linear rigidity. The only requirement for our analysis is that the values Ω_1 and Ω_2 should be close enough and the coupling parameter β is essentially small. The external harmonic excitation acts on the left particle only. A small damping with intensity ν acts at least on the one of the oscillator.

The Hamiltonian of the system may be written in the form

$$H = \sum_{j=1,2} \left(\frac{1}{2}\dot{z}_j^2 + \Omega_j^2 V_j\left(z_j\right) + \frac{\beta}{2} U\left(z_j - z_{3-j}\right) \right) \quad (1)$$

where z_j is the displacement of the j-th particle from its equilibrium position.

3 Two linear oscillators with nonlinear coupling

In this section we assume that the potentials V_j are of the harmonic type:

$$V_j = \frac{1}{2} z_j^2, \quad (2)$$

while the coupling is realized by a nonlinear spring.

In such a case the equations of motion for the forced oscillations can be written as follows

$$\ddot{z}_j + \Omega_j^2 z_j + \beta\, U'(z_j - z_{3-j}) + \nu \dot{z}_j = F(t)\, \delta_{j,1}; \quad F(t) = f \cos \omega t; \quad j = 1, 2. \quad (3)$$

Here $\delta_{j,i}$ is the Kronecker delta, and ν is the coefficient of the viscous damping. The dot over the symbol denotes the derivative with respect to time t, while the prime in the function U means the derivative with respect to the argument.

Due to the linearity of the oscillators in the eq. (3) we can make variables transformation, and consider the evolution of the center of masses and the relative displacements:

$$v = \frac{1}{\sqrt{2}} \left(z_1 + z_2\right), \quad w = \frac{1}{\sqrt{2}} \left(z_1 - z_2\right). \quad (4)$$

In the new variables the system (3) looks as follows

$$\ddot{v} + \Omega_s^2 v + \Omega_d^2 w + \nu \dot{v} = \frac{f \cos(t\omega)}{\sqrt{2}}; \quad (5)$$

$$\ddot{w} + \Omega_s^2 w + \Omega_d^2 v + \sqrt{2}\beta U'\left(\sqrt{2} w\right) + \nu \dot{w} = \frac{f \cos(t\omega)}{\sqrt{2}},$$

where

$$\Omega_s^2 = \frac{1}{2}\left(\Omega_1^2 + \Omega_2^2\right) \quad \Omega_d^2 = \frac{1}{2}\left(\Omega_1^2 - \Omega_2^2\right). \quad (6)$$

Equations (5) can be analysed in the framework of the complex envelope variable approximation (CEVA)[Smirnov and Manevitch(2020)]. We introduce the complex variables:

$$\Psi = \frac{1}{\sqrt{2}} \left(\sqrt{\omega}\, v + \frac{i}{\sqrt{\omega}}\, \dot{v} \right), \quad \Phi = \frac{1}{\sqrt{2}} \left(\sqrt{\omega}\, w + \frac{i}{\sqrt{\omega}}\, \dot{w} \right) \quad (7)$$

where ω is the frequency of the external force and $i^2 = -1$. Assuming $\Psi = \psi e^{-i\omega t}$ and $\Phi = \phi e^{-i\omega t}$ we can perform the averaging of the equations (5) over the the period $2\pi/\omega$ (see Appendix A and [Smirnov and Manevitch(2020)] for details). As the result we get the stationary equations for the complex amplitudes ψ and ϕ.

$$\frac{\omega^2 - \Omega_s^2}{2\omega}\psi - \frac{\Omega_d^2}{2\omega}\phi + \frac{i\nu}{2}\psi = -\frac{f}{4\sqrt{\omega}} \quad (8)$$

$$\frac{\omega^2 - \Omega_s^2 - \tilde{\Omega}_c^2}{2\omega}\phi - \frac{\Omega_d^2}{2\omega}\psi + \frac{i\nu}{2}\phi = -\frac{f}{4\sqrt{\omega}},$$

where

$$\tilde{\Omega}_c^2 = \sum_{k=0}^{\infty} a_k \left(\frac{2}{\omega}\right)^k |\phi|^{2k}. \quad (9)$$

The symbol $\sim$ shows that $\tilde{\Omega}_c$ shifts with the increase of amplitude value in contrast to frequencies Ω_s and Ω_d. It is necessary to give some comments to the equation (9). First of all, the sum on the right hand side of the equation (9) appears from the expansion of function U' into Taylor series on the powers of combination of $\phi + \phi^*$. The coefficients a_k depend on the exact form of function U and the series may be calculated to any desired degree of precision. One can see that the frequency $\tilde{\Omega}_c$ depends on the modulus of function ϕ and actual frequency ω. However, as it follows from definition (7), the next relation is valid:

$$|\phi| = \sqrt{\frac{\omega}{2}} A, \quad (10)$$

where A is the amplitude of the relative motion. Consequently, equation (9) represents the expansion of the frequency $\tilde{\Omega}_c$ into series on powers of amplitude A and does not depend on the frequency ω. This circumstance gives us a very powerful tool for the analysis of the nonlinear systems.

Equations (8) have the evident solution

$$\psi = -\frac{\sqrt{\omega}}{2} \left(f \left(\tilde{\Omega}_c^2 - \Omega_d^2 - i\nu\omega + \Omega_s^2 - \omega^2 \right) \right) \times \quad (11)$$

$$\left(\Omega_d^4 - \left(\Omega_s^2 - \omega(\omega + i\nu) \right) \left(\tilde{\Omega}_c^2 - i\nu\omega + \Omega_s^2 - \omega^2 \right) \right)^{-1}$$

$$\phi = \frac{\sqrt{\omega}}{2} \left(f \left(\Omega_d^2 + i\nu\omega - \Omega_s^2 + \omega^2 \right) \right) \times$$

$$\left(\Omega_d^4 - \left(\Omega_s^2 - \omega(\omega + i\nu) \right) \left(\tilde{\Omega}_c^2 - i\nu\omega + \Omega_s^2 - \omega^2 \right) \right)^{-1}.$$

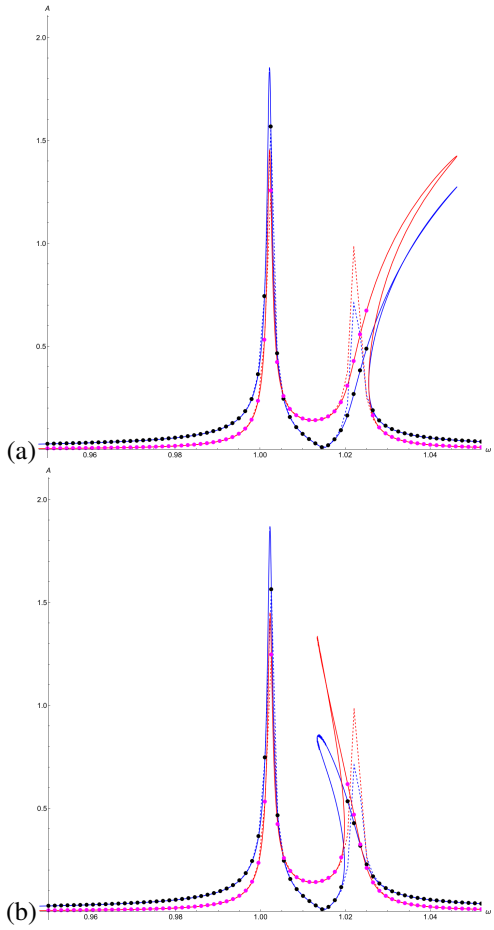

Figure 2. Resonant amplitude-frequency response for the systems with hard (a) and soft (b) nonlinear coupling. Solid lines show the results of the analytical calculations and dots represent the numerical simulation data. Linear system is depicted by dashed lines for reference. The amplitudes of the first particles (excited) are shown in blue, while the red color depicts the amplitude of the second (driven) particle Parameters: $\Omega_1 = 1.0, \Omega_2 = 1.01, \beta = 0.02, \nu = 0.001, f = 0.003$.

The modulus of the second of equations (11) gives us the transcendental equation for the amplitude of the relative motion. On the other hand, we can reverse equations (4) and obtain the expression for the amplitudes of the first and second particles. Let us now discuss the numerical results for the different types of the nonlinearities. Only necessary comment for the understanding of the future results is necessary. As it was shown earlier [Manevitch et al.(2016)Manevitch, Smirnov and Romeo], the eigenfrequency of the pendulum ($V(z) \sim 1-\cos z$) may be obtained in the framework of the CEVA in the closed form as follows (see Appendix A for details):

$$\Omega(A) = \sqrt{\frac{2}{A} J_1(A)}, \tag{12}$$

where J_1 is Bessel function of the first order. If we want to use the hard nonlinear potential ($V(z) \sim \cosh z$), it can be shown that the eigenfrequency is represented as follows:

$$\Omega(A) = \sqrt{\frac{2}{A} I_1(A)}, \tag{13}$$

where I_1 is the modified Bessel function of the first order. Further, we will use expressions (12) and (13) in the analytical calculations.

The results of the analytical calculations in the comparison with the data of the numerical simulations are represented in fig. 2(a) for the hard nonlinearity and in 2(b) for the soft one. The resonance's profiles for the linear system are shown for reference by the dashed lines. The main peculiarity of resonant curves for the nonlinear system consists in the fact that the low-frequency resonant profile does not distinct from the linear one, while the high-frequency peak depends on the nonlinearity essentially. One should note that the presence of only one nonlinear oscillator change the resonant profiles both for the low- and high-frequency peaks [Smirnov(2022)]. The positions of the resonances are determined by the poles of equations (11):

$$\omega_1 = \frac{\sqrt{\Omega_1^2 + \Omega_2^2 + \Omega_c^2 - \sqrt{\Omega_c^4 + (\Omega_1^2 - \Omega_2^2)^2}}}{\sqrt{2}} \tag{14}$$

$$\omega_2 = \frac{\sqrt{\Omega_1^2 + \Omega_2^2 + \Omega_c^2 + \sqrt{\Omega_c^4 + (\Omega_1^2 - \Omega_2^2)^2}}}{\sqrt{2}}.$$

We underline that in the resonant curve of the excited oscillator one of two resonances has the steep asymmetric profile in the vicinity of frequency ω_2 (see Fig. 2). The first of equations (11) shows that some frequency ω_0 with zero oscillation amplitude of the forced oscillator exists, if the damping of the driven oscillator is absent.

$$\omega_0 = \sqrt{\Omega_2^2 + \Omega_c^2/2} \tag{15}$$

The reason of the profile's asymmetry is that, due to changing the phase difference of the oscillators, the driven oscillator effectively quenches the motion of the forced one.

The phase shift between excited and driven oscillators is determined as follows:

$$\delta\theta = \tan^{-1}\left(\frac{\omega\,\nu}{\omega^2 - \Omega_2^2 - \Omega_c^2/2}\right). \tag{16}$$

Looking the at 'nonlinear' part of the resonant curves we can see the the data of the numerical simulations have some discontinues, which correspond to the transitions between stable branches of the solution (11). The frequency of the transition depends on the nonlinearity and the external force amplitude. In order to find the jump's frequency we should return to equations (8). Due to the

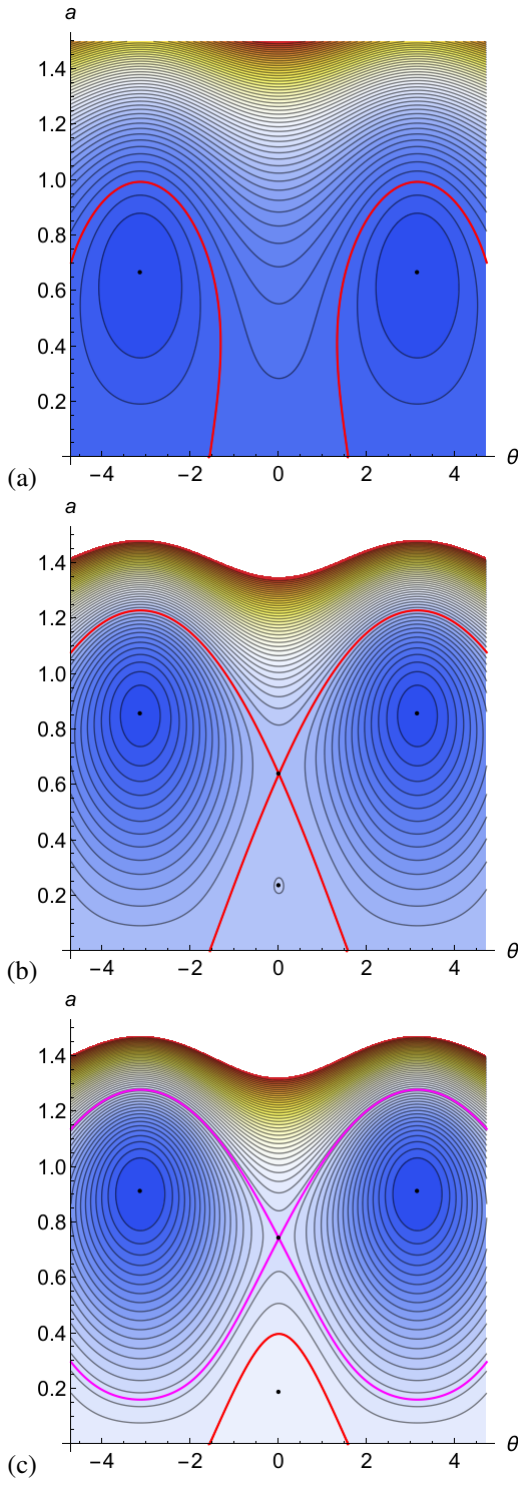

Figure 3. The phase portraits of the equation (18) at the different frequency of the external force. (a) $\omega = 1.025$, (b) $\omega = 1.026$, (c) $\omega = 1.027$.Parameters are $\Omega_1 = 1, \Omega_2 = 1.005, \beta = 0.02$, $f = 0.003$.

linearity of the first one, we can exclude the variable ψ and write the second equation in the form:

$$\left(-\frac{\tilde{\Omega}_c^2}{2\omega} + \frac{\left(\left(\omega^2 - \Omega_s^2\right)^2 - \Omega_d^4\right)}{2\left(\omega^3 - \omega\Omega_s^2\right)}\right)\phi + \frac{f\left(\Omega_d^2 + \Omega_s^2 - \omega^2\right)}{4\sqrt{\omega}\left(\omega^2 - \Omega_s^2\right)} = 0 \tag{17}$$

This equation is associated with the 'slow' (averaged) energy (see Appendix B for detail)

$$E = \frac{(\phi^* + \phi)\left(f\left(\Omega_d^2 + \Omega_s^2 - \omega^2\right)\right)}{4\sqrt{\omega}\left(\omega^2 - \Omega_s^2\right)} + \frac{\left(\left(\omega^2 - \Omega_s^2\right)^2 - \Omega_d^4\right)}{2\left(\omega^3 - \omega\Omega_s^2\right)}|\phi|^2 - \frac{\beta\tilde{U}\left(|\phi|\right)}{2\omega} \tag{18}$$

The fixed points of the energy (18) correspond to the statonary oscillations of the system. Let us define $\phi = ae^{i\theta}$. Considering the phase portrait of the energy (18) on the plane $\{\theta, a\}$ at various frequencies ω, we can control the transition between different types of the oscillations.

Let us discuss the phase portraits of the system (18) for the different frequency values of the external forcing. They are 2π periodic as they depend on the phase shift θ. For the lower values of frequency ω there are two stationary points with phases π and $-\pi$ (see Fig. 3(a)). The limiting phase trajectory (the LPT is the trajectory corresponding to maximum energy exchange with the forcing from zero initial conditions) demonstrated by red line, increases with the frequency growth. The new unstable stationary point, which is crossed by the separatrix, appears at some frequency ω_*. While the frequency increases the separatrix's loop grows and it reaches the axis $a = 0$. At the moment the separatrix coincides with the LPT, and the new branch of LPT solution appears (Fig. 3(b)). The separatrix undergoes the transformation between homoclinic and heteroclinic forms. The amplitudes of the oscillations jump from the high value to the lower one. The LPT, which starts from zero initial conditions, sustains the bifurcation between large and small forms. It corresponds to the low amplitude response of the system (Fig. 3(c)).

4 Double nonlinear system

The system comprising one nonlinear oscillator has been considered in [Smirnov(2022)] with detailed analysis of the resonant behaviour and its stability. In the section, we study two nonlinear oscillators that are coupled by the linear spring. For convenience, we write the hamiltonian (1) in the form:

$$H = \sum_{j=1,2}\left(\frac{1}{2}\dot{z}_j^2 + \Omega_j^2 V_j\left(z_j\right) + \frac{\beta}{2}z_j z_{3-j}\right), \tag{19}$$

Introducing the complex variables Ψ_1 and Ψ_2 and following the complexification procedure discussed above (see Appendix A for detail), we get the stationary equations for the complex amplitudes ψ_1 and ψ_2:

$$\frac{\omega}{2}\psi_j - \frac{\tilde{\Omega}_j^2}{2\omega}\psi_j - \frac{\beta}{2\omega}\psi_{3-j} + \frac{1}{2}i\nu\psi_j = -\frac{f}{2\sqrt{2\omega}}\delta_{j,1}, \tag{20}$$

where values $\tilde{\Omega}_j$ are associated with the respective oscillator and they depend on the oscillation amplitude similarly equation (9).

We have obtained the equations for the non-linear system in the form, that formally coincides with the equations for the linear one. Therefore, we can write the solution for equations (20) immediately:

$$\psi_1 = \sqrt{\frac{\omega}{2}}\,\frac{\left(\tilde{\Omega}_2^2 - \omega\,(\omega + i\nu)\right) f}{D} \tag{21}$$
$$\psi_2 = -\sqrt{\frac{\omega}{2}}\,\frac{\beta f}{D},$$
$$D = \left(\left(i\nu\omega + \omega^2 - \tilde{\Omega}_1^2\right)\left(i\nu\omega + \omega^2 - \tilde{\Omega}_2^2\right) - \beta^2\right).$$

Formally, the solution obtained coincides with its linear analogue. Therefore, the main peculiarities of the resonant curves in the nonlinear system look alike the linear ones. Zero-amplitude frequency in the absence of the damping is

$$\omega_0 = \tilde{\Omega}_2,$$

the oscillators phase difference can written as follows

$$\theta = tan^{-1}\left(\frac{\nu\,\omega}{\omega^2 - \tilde{\Omega}_2^2}\right),$$

and it undergoes the discontinuity with the value jump of magnitude π just as it appears in the linear analogue (16). One should note that the amplitude of the driven oscillator at the zero-amplitude frequency can be determined as

$$A_2 = \sqrt{\frac{2}{\omega}}\frac{f}{\beta}.$$

Therefore, we can write

$$\omega_0 = \tilde{\Omega}_2\left(\frac{f}{\beta}\right)$$

Equations (21) are transcendental and they should be solved with use of a numerical procedure. Generally speaking, finding solution for such a system is not a simple task, particularly, taking into account the existence of the multiple branches of the nonlinear frequencies $\tilde{\Omega}_j$. Nevertheless, due to the relative simplicity of equations (21), they may be reduced to one equation with respect to amplitude of the first oscillator only. In such a case the respective numerical procedure is facilitated essentially (see Appendix C).

Fig. 4 shows the amplitude-frequency relations for the system, with two nonlinear oscillators, both of the 'soft' type ($V(z) \sim 1 - \cos z$). The amplitudes of the excited and driven oscillators are depicted in blue and red, respectively. The influence of the nonlinearity is significant for both resonant peaks. Therefore, the effect of the bistability [Kivshar(2018); Miroshnichenko et al.(2010)Miroshnichenko, Flach and Kivshar] appears in 'low-' as well as in the 'high'-frequency domains. The bistability is caused by the presence of several branches of the solution for equation (21). In practice, if the numerical simulation starts with zero initial conditions, the system chooses only one of three possible stationary amplitudes. It is seen that the numerical solution demonstrates sudden hopping from one stable branch of the solution to another when the frequency grows.

Fig. 5 shows the resonant curves for the the system with the nonlinearity of the hard type: $V(z) \sim \cosh z$. There are two pairs of the solutions of the amplitude-frequency response. The figure demonstrates the fact, that there are two resonant manifolds; each of them gives a stationary solution for the forced system. However, the solutions are quite close and can be barely resolved in the analysis of the numerical solutions. Only for the high-frequency response the solution with lower amplitude is realized numerically. We see the significant effect of the nonlinearity on the amplitude of the forced oscillator.

In the Fig. 6 we present the amplitude-frequency response for the case when one of the oscillators is of the 'soft' type while the second one is of the 'hard' type. We again demonstrate the solutions belonging to two different resonant manifolds, which correspond to the two pairs of the solutions. The main intriguing feature of the solutions is that during the numerical verification of the results we observe not only hopping between the branches of the same bistable solutions. We can also see the switch between the solutions belonging to different resonant manifolds. This fact makes almost impossible to represent the evolution of the system on the phase plane representing the resonant manifold, as it was done in the previous section. However, the form of the numerical solutions response and a very good agreement with the results of the asymptotic analysis shows that the two pairs of the solutions are not the artefact of the analysis procedure, rather then new phenomenon observed in the phase space.

5 Conclusion

In this work we continued the consideration of the classical and very simple analogues to the Fano resonance on the example of two coupled oscillators with the nonlinearity of the 'soft' as well as 'hard' types. The oscillator excited by the external forcing can be interpreted as associated with the continuum state of the quantum mechanical system, while the driven oscillator can play the

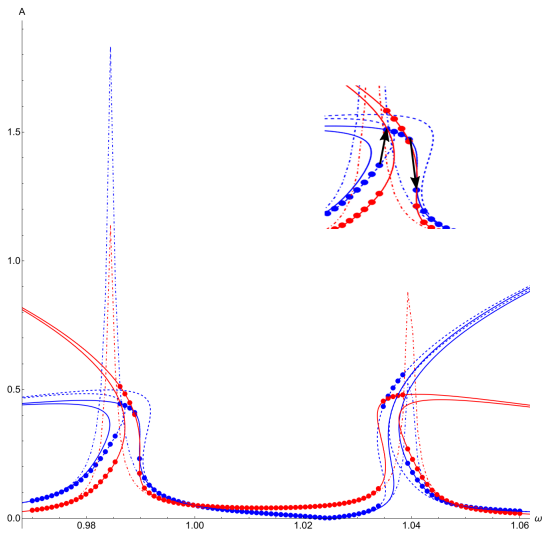

Figure 6. The same as in Fig.4 for the system with the hard and soft nonlinearity ($V_1(z) \sim \cosh z; V_2(z) \sim 1 - \cos z$). Insert shows the jumps between branches of different roots (left arrow) and the same ones (right arrow). See text for explanation. Parameters: $\Omega_1 = 1.0$, $\Omega_2 = 1.0247$, $\beta = 0.05$, $\nu_1 = 0.001$, $\nu_2 = 0.001$, $f = 0.005$.

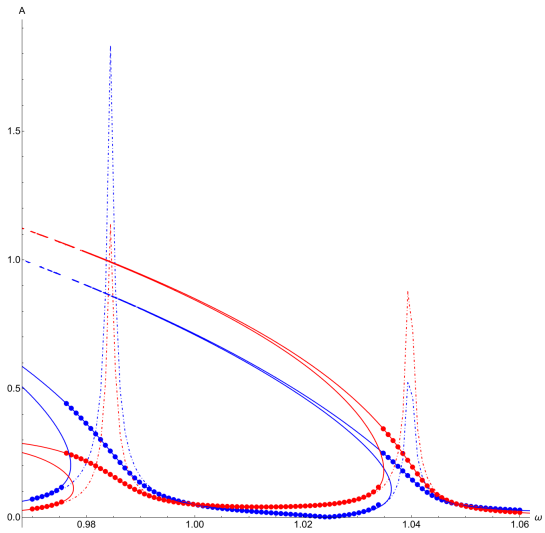

Figure 4. Anti-resonance in the system with the soft nonlinearity of the oscillators ($V(z) \sim 1 - \cos z$). The amplitudes of the excited and driven oscillators calculated from the equation (21) are depicted in blue and red, respectively. The blue and red circles show the data of the direct numerical simulations for the excited and driven oscillators, respectively. Dot-dashed lines show the reference linear system. Parameters: $\Omega_1 = 1.0$, $\Omega_2 = 1.0247$, $\beta = 0.05$, $\nu_1 = 0.001$, $\nu_2 = 0.001$, $f = 0.01$.

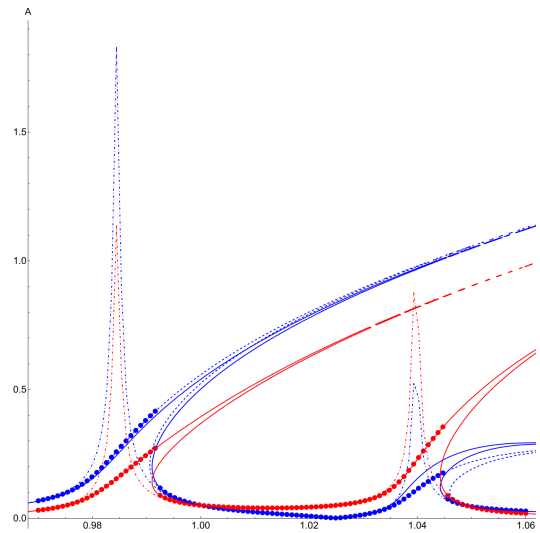

Figure 5. The same as in Fig.4 for the system with the hard nonlinearity ($V(z) \sim \cosh z$). Parameters: $\Omega_1 = 1.0$, $\Omega_2 = 1.0247$, $\beta = 0.05$, $\nu_1 = 0.001$, $\nu_2 = 0.001$, $f = 0.005$.

role of the leaky discrete state. With help of the well developed procedure of the complex envelope variable approximation we obtain the closed expressions for the oscillators' amplitudes without any additional limitations on the value of the nonlinearity. The representation of the solutions is not explicit as the equations themselves are the transcendental equations for the amplitudes with the nonlinearity, which represents the natural oscillation frequency of oscillators. It is convenient that the form of the equations is the same for the linear and nonlinear systems. This finding has the intimate physical meaning: the resonant curve has a universal shape, if the resonant frequency is considered as the frequency of natural oscillations of a given amplitude.

The system of two linear oscillators with nonlinear coupling demonstrates several branches of the amplitude-frequency relation, which results in the transition between different stationary solutions at some values of the frequency of the external force. We reveal that the mentioned above transitions can be associated with the bifurcations of the separatrix passing through the unstable stationary state. The separatrix transforms from homoclinic to heteroclinic forms. Simultaneously the limiting phase trajectory, which starts from zero initial conditions, sustains the bifurcation between large and small forms. In the numerical solutions of the system of two linear oscillators we observe two resonant peaks with switching between the different branches of the resonant response. The bistability of the stationary states exists in the vicinity of the resonant frequencies even for the systems, where only one of the oscillators is nonlinear [Smirnov(2022)]. However, in our work we demonstrate the hopping between the different branches of the solution in the case of the linear oscillators and nonlinear coupling.

The case when both of the oscillators are nonlinear while the coupling is linear, yields even more interesting phenomenon. In the numerical analysis we see again the two resonant frequency areas. However, there are two resonant manifolds each of them having stationary solu-

ical modelling of the initial system demonstrates jumps between the branches of the same bistable solution as well as switches between the different solutions belonging to different resonant manifolds. Our analysis reveals the transitions explaining the unusual form of the amplitude-frequency curves.

We have not discussed the stability problem because the procedure does not differ from that discussed in the previous work and it may be performed necessarily.

Appendix

A. Complexification of the equations of motion

The equations of motions for the system with hamiltoian (19) are read

$$\ddot{z_j} + \Omega_j^2 V_j'(z_j) + \beta z_{3-j} + \nu \dot{z_j} = f \cos \omega t \ \delta_{j,1}$$

Introducing the complex variables Ψ_j (see equations (7)), we can write

$$i\frac{d\Psi_j}{dt} - \frac{\omega}{2}\left(\Psi_j - \Psi_j^*\right) - \frac{\Omega_j^2}{\sqrt{2\omega}} V'\left(\frac{1}{\sqrt{2\omega}}\left(\Psi_j + \Psi_j^*\right)\right) + i\frac{\nu}{2}\left(\Psi_j - \Psi_j^*\right) - \beta\left(\Psi_{3-j} + \Psi_{3-j}^*\right) = \frac{f\left(e^{-i\omega t} + e^{i\omega t}\right)}{2\sqrt{2\omega}}\delta_{j,1}$$

We assume $V'(z) = \sin z$ and expand it into series on the order of the argument:

$$V_j' = \sum_{k=0}^{\infty}\sum_{n=0}^{2k+1} \frac{(-1)^k}{(2k+1-n)!n!}\left(\frac{1}{\sqrt{2\omega}}\right)^{2k+1} \Psi^{2k+1-n}\Psi^{*n}$$

Choosing $\Psi_j = \psi_j e^{-\omega t}$, where ψ_j does not depend on time t, we can multiply the equation on factor $e^{i\omega t}$ and perform the averaging over the period $T = 2\pi/\omega$. After the averaging we get

$$V' = \sum_{k=0}^{\infty} \frac{(-1)^k}{(k+1)!k!}\left(\frac{1}{\sqrt{2\omega}}\right)^{2k+1} \psi^{k+1}\psi^{*k} = J_1\left(\frac{2}{\omega}|\psi_j|\right)\frac{\psi_j}{|\psi_j|}$$

where J_1 is the Bessel function of the first order. Taking into account relation (17) and choosing

$$\tilde{\Omega}_j^2 = \Omega_j^2 \frac{2}{A} J_1(A)$$

we obtaine equations (20).

B. Average slow time hamiltonian

In order to analys the phase portrait of the nonlinear system, it is convenient to formulate the energy function in terms of complex envelopes ψ_j. Let us to define the complex variables and substitute them into hamiltonian (19). Expanding the different terms into series, we obtaine

$$H = \sum_{j=1,2}(-\frac{\omega}{2}\left(\Psi_j - \Psi_j^*\right)^2 + \frac{\beta}{4\omega}\left(\Psi_j + \Psi_j^*\right)\left(\Psi_{3-j} + \Psi_{3-j}^*\right) + \Omega_j^2 \sum_{k=0}^{\infty} a_k^{(j)}\left(\frac{1}{\sqrt{2\omega}}\right)^k \sum_{n=0}^{k} C_n^k \Psi_j^{k-n}\Psi_j^{*n})$$

where $a_k^{(j)}$ are the expansion's coefficients for function V_j and C_n^k are the polinomial coefficients. In the case of the forced oscillations we need in the work of the external force:

$$W = f\cos\omega t z_1 = f\frac{\left(e^{-i\omega t} + e^{i\omega t}\right)}{2\sqrt{2\omega}}\left(\Psi_1 + \Psi_1^*\right)$$

Averaging the hamiltonian over the period $T = 2\pi/\omega$ and substracting the energy of the carrier $\omega\left(|\psi_1|^2 + |\psi_2|^2\right)$, we get the "slow" hamiltonian in the terms of the complex envelopes [Smirnov and Manevitch(2020)].

C. Reduction of the system transcendental equations

To reduce the complexity of equations (21) for the numerical search of roots, one needs to consider the oscillations' amplitudes using relation (10). Calculating the module of equations (21), we get two real equations, which can be solved with respect to amplitude A_2 and nonlinear frequency $\tilde{\Omega}_2$.

$$A_2 = A_2\left(A_1, \tilde{\Omega}_1(A_1)\right)$$
$$\tilde{\Omega}_2 = \tilde{\Omega}_2\left(A_1, \tilde{\Omega}_1(A_1)\right)$$

It is important that the solution obtained has two roots. Next step is to exclude the amplitude A_2 from the equation for the amplitude A_1. Using the explicit form of frequency $\tilde{\Omega}_2$ in the expression for amplitude A_1, we should substitute amplitude $A_2\left(A_1, \tilde{\Omega}_1(A_1)\right)$ into it. Thus we obtain the closed expression, which contains the amplitude A_1 only. The results of such numerical solutions are represented in Figs 4 - 6.

Conflict of interest The authors declare no conflicts of interest.

Acknowledgements This work was supported by Program of Fundamental Researches of the Russian Academy of Sciences (project no. FFZE-2022-0009)

References

Albu-Schäffer, A., Della Santina, C., 2020. A review on nonlinear modes in conservative mechanical systems. Annual Reviews in Control 50, 49–71. doi:https://doi.org/10.1016/j.arcontrol.2020.10.002.

Beutler, H., 1935. Über absorptionsserien von argon, krypton und xenon zu termen zwischen den beiden ionisierungsgrenzen $^2p_3^{2/0}$ und $^2p_1^{2/0}$. Zeitschrift für Physik 93, 177 – 196. doi:10.1007/BF01365116.

Fano, U., 1935. Sullo spettro di assorbimento dei gas nobili presso il limite dello spettro d'arco. Nuovo Cimento 12, 154 – 161.

Fano, U., 1961. Effects of configuration interaction on intensities and phase shifts. Phys. Rev. 124, 1866 – 1878.

Joe, Y., Satanin, A., Kim, C., 2006. Classical analogy of fano resonances. Phys. Scr. 74, 259 – 266. doi:10.1088/0031-8949/74/2/020.

Kim, G., Lee, S.B., Kim, T.S., Ihm, J., 2005. Fano resonance and orbital filtering in multiply connected carbon nanotubes. Rhys Rev B 71, 205415. doi:10.1103/PhysRevB.71.205415.

Kivshar, Y., 2018. Energy localization, fano resonances, and nonlinear meta-optics. Low Temperature Physics 44, 726. doi:10.1063/1.5041440.

Koroleva(Kikot), I., Kosevich, Y., 2023. Effects of nonlinearity and a new nonlinear resonance in two-path phonon transmittance in lattices with two-dimensional arrays of atomic defects. Phys Rev E 107, 054217. doi:0.1103/PhysRevE.107.054217.

Kosevich, Y.A., 2008. Multichannel propagation and scattering of phonons and photons in low-dimension nanostructures. Phys.– Usp. 51(8), 848. doi:10.1070/PU2008v051n08ABEH006597.

Kovaleva, M.A., Manevitch, L.I., Romeo, F., 2019. Stationary and non-stationary oscillatory dynamics of the parametric pendulum. Communications in Nonlinear Science and Numerical Simulation 76, 1.

Kroner, M., Govorov, A., Remi, S., et al., 2008. The nonlinear fano effect. Nature 451, 311 – 314. doi:10.1038/nature06506.

Lebedev, M., Misochko, O., 2022. On the question of a classical analog of the fano problem. Physics, Uspekhi 65, 627 —- 640. doi:10.3367/UFNe.2021.11.039098.

Manevitch, L., 2007. New approach to beating phenomenon in coupled nonlinear oscillatory chains. Arch. Appl. Mech. 77, 301. doi:10.1007/s00419-006-0081-1.

Manevitch, L., Smirnov, V., Romeo, F., 2016. Non-stationary resonance dynamics of the harmonically forced pendulum. Cybernetics and Physics 5, 91 – 95.

Manevitch, L.I., Smirnov, V.V., 2010. Limiting phase trajectories and the origin of energy localization in nonlinear oscillatory chains. Phys. Rev. E 82, 036602.

M.F., L., Rybin, M., Poddubny, A., Kivshar, Y., 2017. Fano resonances in photonics. Nature Photonics 11, 543. doi:10.1038/NPHOTON.2017.142.

Miroshnichenko, A., 2009. Instabilities and quasi-localized states in nonlinear fano-like systems. Physics Letters A 373, 3586 – 3590. doi:10.1016/j.physleta.2009.02.079.

Miroshnichenko, A., Flach, S., Kivshar, Y., 2010. Fano resonances in nanoscale structures. Rev. Mod. Phys. 82, 2257 – 2298. doi:10.1103/RevModPhys.82.2257 PA.

Neishtadt1, A.I., Vasiliev, A.A., Artemyev, A.V., 2013. Capture into resonance and escape from it in a forced nonlinear pendulum. Regular and Chaotic Dynamics 18, 691–701.

Perchikov, N., Gendelman, O.V., 2024. Transient dynamics in strongly nonlinear systems: Optimization of initial conditions on the resonant manifold. Philosophical Transactions A 181, 114661.

Riffe, D., 2011. Classical fano oscillator. Phys. Rev. B 84, 064308. doi:10.1103/PhysRevB.84.064308.

Savin, A., Kivshar, Y., 2017. Phononic fano resonances in graphene nanoribbons with local defects. Scientific Reports 7, 4668. doi:10.1038/s41598-017-04987-w.

Smirnov, V., 2022. Fano resonance in the essentially nonlinear classic system. Int.J. Nonlinear Mechanics 142, 104015. doi:10.1016/j.ijnonlinmec.2022.104015.

Smirnov, V., Manevitch, L., 2020. Complex envelope variable approximation in nonlinear dynamics. Rus. J. Nonlin. Dyn. 16(3), 491 – 515. doi:10.20537/nd200307.

Usik, E., Amelina, N., Fradkov, A.L., 2024. Feedback resonance in fermi–pasta–ulam chain. Chaos, Solitons and Fractals 181, 20170131. doi:https://doi.org/10.1016/j.chaos.2024.114661.

Wang, Q., Huang, Y., Yao, Z., Xu, X., 2016. Analysis of transition from lorentz resonance to fano resonance in plasmon and metamaterial systems. Opt Quant Electron 48, 83. doi:10.1007/s11082-015-0358-0.

Xu, H., Zhao, M., Chen, Z., et al, 2018. Sensing analysis based on tunable fano resonance in terahertz graphene-layered metamaterials. J Appl Phys 123, 203103. doi:10.1063/1.5029546.